

Published in final edited form as:

*J Biomech.* 2009 May 11; 42(7): 938–944. doi:10.1016/j.jbiomech.2008.07.039.

## Theoretical analysis of alendronate and risedronate effects on canine vertebral remodeling and microdamage

Xiang Wang<sup>a</sup>, Antonia M. Erickson<sup>a</sup>, Matthew R. Allen<sup>b</sup>, David B. Burr<sup>b,c</sup>, R. Bruce Martin<sup>a</sup>, and Scott J. Hazelwood<sup>d,\*</sup>

<sup>a</sup>Lawrence J. Ellison Musculoskeletal Research Center, University of California Davis Medical Center, Sacramento, CA 95817, USA

<sup>b</sup>Department of Anatomy and Cell Biology, Indiana University School of Medicine, Indianapolis, IN 46202, USA

<sup>c</sup>Department of Orthopaedic Surgery, Indiana University School of Medicine, Indianapolis, IN 46202, USA

<sup>d</sup>Biomedical and General Engineering Department, California Polytechnic State University, San Luis Obispo, CA 93407

### Abstract

Bisphosphonates suppress bone remodeling activity, increase bone volume, and significantly reduce fracture risk in individuals with osteoporosis and other metabolic bone diseases. The objectives of the current study were to develop a mathematical model that simulates control and 1 year experimental results following bisphosphonate treatment (alendronate or risedronate) in the canine fourth lumbar vertebral body, validate the model by comparing simulation predictions to 3 year experimental results, and then use the model to predict potential long term effects of bisphosphonates on remodeling and microdamage accumulation. To investigate the effects of bisphosphonates on bone volume and microdamage, a mechanistic biological model was modified from previous versions to simulate remodeling in a representative volume of vertebral trabecular bone in dogs treated with various doses of alendronate or risedronate, including doses equivalent to those used for treatment of post-menopausal osteoporosis in humans. Bisphosphonates were assumed to affect remodeling by suppressing basic multicellular unit activation and reducing resorption area. Model simulation results for trabecular bone volume fraction, microdamage, and activation frequency following 1 year of bisphosphonate treatment are consistent with experimental measurements. The model predicts that trabecular bone volume initially increases rapidly with 1 year of bisphosphonate treatment, and continues to slowly rise between 1 and 3 years of treatment. The model also predicts that microdamage initially increases rapidly, 0.5 to 1.5-fold for alendronate or risedronate during the first year of treatment, and reaches its maximum value by 2.5 years before trending downward for all dosages. The model developed in this study suggests that increasing bone volume fraction with long

\*Please address all correspondence to: Scott J. Hazelwood, PhD, Biomedical and General Engineering Department, California Polytechnic State University, San Luis Obispo, CA 93407, Phone: 1-805-756-6304, Fax: 1-805-756-6424, Email: shazelwo@calpoly.edu.

**Conflict of interest statement:** MRA and DBB have received financial support from Eli Lilly, The Alliance for Better Bone Health (Procter and Gamble), and Amgen. In addition, DBB serves as an advisor for Eli Lilly and Merck, and as a speaker for Eli Lilly, The Alliance for Better Bone Health, Amgen, Roche, and GlaxoSmithKline. XW, AME, RBM, and SJH disclose that they do not have conflicts of interest regarding the work presented in this manuscript.

**Publisher's Disclaimer:** This is a PDF file of an unedited manuscript that has been accepted for publication. As a service to our customers we are providing this early version of the manuscript. The manuscript will undergo copyediting, typesetting, and review of the resulting proof before it is published in its final citable form. Please note that during the production process errors may be discovered which could affect the content, and all legal disclaimers that apply to the journal pertain.

term bisphosphonate treatment may sufficiently reduce strain and damage formation rate so that microdamage does not accumulate above that which is initiated in the first two years of treatment.

## Keywords

Bisphosphonate; bone remodeling; BMU; alendronate; risedronate; simulation; canine; microdamage

## Introduction

Bisphosphonates (BPs) are anti-resorptive drugs that suppress bone remodeling, increase bone volume and bone mineral density, and are used to treat post-menopausal osteoporosis and other bone fragility disorders (Rodan and Fleisch, 1996; Chavassieux *et al.*, 1997; Tonino *et al.*, 2000; Ding *et al.*, 2003; Dufresne *et al.*, 2003; Recker *et al.*, 2005). At the tissue level in humans, BP treatment is associated with decreased bone resorption and turnover (Storm *et al.*, 1993; Rodan and Fleisch, 1996; Eriksen *et al.*, 2002) and therefore provides a transient increase in bone volume (filling of pre-existing remodeling spaces). This may be followed by a further trend to increase bone volume by reducing the amount of bone resorbed relative to that formed by basic multicellular units (BMUs) (Boyce *et al.*, 1995). In post-menopausal women, BPs reduce fracture risk by improving the structural properties of bone (Delmas, 2000) and increasing the degree of mineralization (Boivin *et al.*, 2000). However, BP treatment also results in significant microdamage accumulation and a reduction in bone toughness in canine vertebrae (Mashiba *et al.*, 2001; Komatsubara *et al.*, 2003; Allen *et al.*, 2006; Allen and Burr, 2007). The microdamage accumulation is due, at least in part, to decreased remodeling, which is the only mechanism in bone to remove fatigue damage (Burr *et al.*, 1985; Mori and Burr, 1993). These observations, some having positive and others negative implications in bone, indicate the need for a better understanding of BP effects on bone remodeling, structure, and material properties.

While long term BP studies have focused on alterations to bone mineral density and bone turnover (Miller *et al.*, 1997; Tonino *et al.*, 2000; Bone *et al.*, 2004; Ste-Marie *et al.*, 2004; Borah *et al.*, 2006; Zoehrer *et al.*, 2006), their effects on microdamage accumulation have not been studied beyond three years of treatment (Forwood *et al.*, 1995; Hirano *et al.*, 2000; Mashiba *et al.*, 2000; Mashiba *et al.*, 2001; Komatsubara *et al.*, 2003; Day *et al.*, 2004; Komatsubara *et al.*, 2004; Mashiba *et al.*, 2005; Allen *et al.*, 2006; Allen and Burr, 2007). Results from canine studies have documented microdamage increases in the vertebral body, rib, and ilium following 1 to 3 years of BP treatment, but these changes were compensated for by increases in bone mass and structural properties, including ultimate load and stiffness (Allen and Burr, 2007). However, some of these studies also documented significant reductions in bone toughness, the intrinsic ability of the tissue to resist fracture. Since BP treatment in patients with osteoporosis now extends 10 years or more, the long term effects of BPs on microdamage accumulation and bone fragility are of clinical interest.

In the present study, we develop a mathematical model to explore the long term effects of BP treatment on bone. We have previously developed computational models simulating bone mechanics and remodeling in a representative volume of bone (Martin, 1995; Hazelwood *et al.*, 2001; Nyman *et al.*, 2004; Nyman *et al.*, 2006). These models simulate BMU activation and remodeling in response to mechanical loading and fatigue microdamage. Our overall goal in developing these mathematical models is to simulate the long term effects of BPs on remodeling and microdamage accumulation in current animal models and, ultimately, in humans. As an initial step, our approach in the current study is to develop a model of remodeling in a representative volume of trabecular bone based on control and 1 year experimental results

following BP treatment in the canine fourth lumbar vertebral body (Allen *et al.*, 2006), and subsequently to test its predictions against data from a 3 year alendronate study (Allen and Burr, 2007). Then, in an effort to understand long term bisphosphonate treatment effects over periods similar to those for clinical use in humans, we examine model predictions after 10 years of simulated treatment.

## Methods

The control and 1 year data used for model development were from skeletally mature female beagles treated daily with saline vehicle or one of three doses of alendronate (ALN: 0.10, 0.20, or 1.00 mg/kg/day) or risedronate (RIS: 0.05, 0.10, or 0.50 mg/kg/day) (Allen *et al.*, 2006). The middle doses of ALN and RIS correspond to the clinical treatment dose, on a mg/kg basis, for post-menopausal osteoporosis. The lower dose of ALN corresponds to the preventative dose for osteoporosis, while the higher dose of both ALN and RIS are approximately equivalent to those used for treatment of Paget's disease. In that study, trabecular bone mineral density (BMD, g/cm<sup>3</sup>), volume fraction (BV/TV), activation frequency (Ac.f), and microdamage (crack surface density or Cr.S.Dn) in the fourth lumbar vertebra (L4) were quantified.

A previous bone remodeling algorithm (Hazelwood *et al.*, 2001; Nyman *et al.*, 2004) was modified to simulate remodeling in a 1 cm<sup>3</sup> volume of canine L4 vertebral trabecular bone under uniaxial cyclic loading. The model describes histomorphometric variables governing bone mechanical properties (Table 1). The cancellous bone structure was assumed to be isotropic with a uniform bone volume fraction, BV/TV. The continuum-level elastic modulus (E) was assumed to be related to BV/TV by

$$E=E_0(BV/TV)^b, \quad (1)$$

where  $E_0 = 19,735$  MPa and  $b = 2.4217$  were obtained by fitting experimental data from control and 1 year BP-treated dogs to Eq. 1 (Table 2). Peak strain was calculated as

$$\varepsilon = \sigma / E, \quad (2)$$

where  $\sigma$  is the peak stress applied during cyclic loading.

A loading potential,  $\Phi$ , was defined to characterize the mechanical environment as it affects remodeling (Hazelwood *et al.*, 2001):

$$\Phi = R_L \varepsilon^q, \quad (3)$$

where  $R_L$  is the loading frequency (assumed to be constant at 3000 cycles per day), and  $q = 4$  adjusts the relative contribution of peak strain and loading frequency to the loading potential.

## Microdamage

Microdamage (Cr.S.Dn) was defined as cumulative microcrack length per unit cross-sectional area of bone (mm/mm<sup>2</sup>). The damage formation rate was assumed to be proportional to the loading potential,

$$\left(\frac{dCr.S.Dn}{dt}\right)_F = k_D \Phi, \quad (4)$$

where  $k_D$  is chosen to make the damage formation and removal rates equal under steady state conditions (Hazelwood *et al.*, 2001).

The fatigue microdamage removal rate was modeled as (Martin, 1995)

$$\left(\frac{dCr.S.Dn}{dt}\right)_{Rs} = Cr.S.Dn \cdot Ac.f \cdot Rs.Ar \cdot F_s, \quad (5)$$

where  $Ac.f$  is the BMU activation frequency,  $Rs.Ar$  is the resorption space area, and  $F_s$  is a “steering factor” to account for targeted damage removal (Martin, 1985). Hence, the net damage accumulation rate is

$$\frac{dCr.S.Dn}{dt} = \left(\frac{dCr.S.Dn}{dt}\right)_F - \left(\frac{dCr.S.Dn}{dt}\right)_{Rs}. \quad (6)$$

### Bone volume fraction

The time rate of change of bone volume fraction,  $d(BV/TV)/dt$ , was assumed to be a function of the mean bone resorption ( $Rs.Ar/Rs.P$ ) and refilling ( $FAr/FP$ ) rates within individual BMUs, and the mean densities of resorbing ( $N.Rs.BMU$ ) and refilling ( $N.F.BMU$ ) BMUs (Martin, 1985):

$$\frac{d(BV/TV)}{dt} = \frac{FAr}{FP} \cdot N.F.BMU - \frac{Rs.Ar}{Rs.P} \cdot N.Rs.BMU, \quad (7)$$

$$N.F.BMU = \int_{t-(Rs.P+Rv.P+FP)}^{t-(Rs.P+Rv.P)} Ac.f \, dt', \quad (8)$$

$$N.Rs.BMU = \int_{t-Rs.P}^t Ac.f \, dt', \quad (9)$$

where  $Rs.Ar$  and  $FAr$  are the mean resorption and refilling areas and  $Rs.P$  and  $FP$  are the mean resorption and refilling periods, respectively, of individual BMUs (Table 2). The shape of the BMU resorption cavity was modeled as a semi-ellipse having a mean cross-sectional area of  $0.014 \text{ mm}^2$  as measured from the control dogs (previously unpublished data (Allen *et al.*, 2006)).

### BMU activation frequency

BMU  $Ac.f$  ( $\text{BMUs}/\text{mm}^2/\text{day}$ ) was assumed to be a function of disuse, microdamage, and the available surface area for remodeling,  $BS/TA$ . This leads to the equation

$$Ac.f = (Ac.f_{\text{damage}} + Ac.f_{\text{disuse}}) \frac{BS/TA}{(BS/TA)_{\text{max}}}, \quad (10)$$

$$Ac.f_{\text{damage}} = \begin{cases} \frac{Ac.f_0 \cdot Ac.f_{\text{max}}}{Ac.f_0 + (Ac.f_{\text{max}} - Ac.f_0) \cdot \exp(k_r \cdot Ac.f_{\text{max}} \cdot (Cr.S.Dn - Cr.S.Dn_0) / Cr.S.Dn_0)} & Cr.S.Dn > Cr.S.Dn_0 \\ Ac.f_0 \cdot (Cr.S.Dn / Cr.S.Dn_0) & Cr.S.Dn \leq Cr.S.Dn_0 \end{cases}, \quad (11)$$

$$Ac.f_{\text{disuse}} = \begin{cases} \frac{Ac.f_{\text{max}}}{1 + \exp(k_b \cdot (\Phi - k_c))} & \Phi < \Phi_0 \\ 0 & \Phi \geq \Phi_0 \end{cases}, \quad (12)$$

where  $Ac.f_{\text{damage}}$  and  $Ac.f_{\text{disuse}}$  represent the BMU activation frequencies associated with microdamage and disuse, respectively, and are assumed to be independent remodeling responses. Specific surface area was determined from BV/TV using an empirical relationship,

$$\begin{aligned} BS/TA &= 32.3(1 - BV/TV) - 93.9(1 - BV/TV)^2 + 134(1 - BV/TV)^3 \\ &\quad - 101(1 - BV/TV)^4 + 28.8(1 - BV/TV)^5 \end{aligned} \quad (13)$$

normalized by the maximum value,  $(BS/TA)_{\text{max}} = 4.191 \text{ mm}^{-1}$  (Hazelwood *et al.*, 2001).

To compare simulation predictions with experimental results, the annual activation frequency ( $Ac.f_{\text{year}}$ , BMU/year) was calculated as (Nyman *et al.*, 2004)

$$Ac.f_{\text{year}} = 365 \cdot \frac{Md.S.Le \cdot Ac.f}{BS/TA}, \quad (14)$$

where  $Md.S.Le$  is the mean mineralized length of a BMU's active surface (Table 2).

### Bisphosphonate effects

BP treatment was assumed to (1) suppress BMU activation frequency (Storm *et al.*, 1993; Chavassieux *et al.*, 1997; Chavassieux *et al.*, 2000; Eriksen *et al.*, 2002) and (2) reduce resorption cavity depth (Boyce *et al.*, 1995). A potency variable,  $P$ , was defined to quantify the BP's ability to suppress remodeling activation (Nyman *et al.*, 2004):

$$P = P_{\text{max}}(1 - \exp(-\tau_s \cdot N.Rs.BMU)), \quad (15)$$

where  $N.Rs.BMU$  is the number of resorbing BMUs,  $P_{\text{max}} = 1$  is the fully suppressed potency, and  $\tau_s$  is a suppression coefficient (Table 3). The activation frequency was suppressed by multiplying  $Ac.f$  by  $(1-P)$ , where  $P$  has a value between 0 and 1. Resorption cavity area ( $Rs.Ar$ ) was also assumed to be reduced, depending on the type and dosage of BP treatment (Nyman *et al.*, 2004). A refilling coefficient describing the balance between bone formed and resorbed at each resorption site was defined as

$$C_F = \frac{F_{Ar}}{R_s \cdot Ar_{(BP)}}, \quad (16)$$

where  $R_s \cdot Ar_{(BP)}$  is the reduced resorption cavity area dependent on the BP administered and dosage (Table 2).

### Numerical Simulation

All simulations were performed in MATLAB (MathWorks, Natick, MA). The model was implemented using a time step of 1 day. An equilibrium status of trabecular bone remodeling that matched the experimental control data for canine vertebral trabecular bone was obtained first (Table 4). For a BV/TV of 22.3% (Allen *et al.*, 2006) in a 1 cm<sup>3</sup> representative volume of trabecular bone, it was found that a peak cyclic stress of  $\sigma = 0.265$  MPa produces steady state values for the principal outcome variables Ac.f, Cr.S.Dn, and BV/TV similar to the remodeling data of the control dogs. Then, using the equilibrium condition as the baseline, the model was used to find values of the bisphosphonate variables  $\tau_s$  and  $C_F$  that matched the 1 year canine experimental data (Tables 3 and 4). Because BPs suppress bone turnover soon after treatment initiation (Porras *et al.*, 1999), their effects were assumed to begin immediately.

The simulation then was carried out for 3 years of BP treatment and results were compared to recent 3 year experimental data available for the fourth lumbar vertebral body in canines at the middle (0.20 mg/kg/day) and high (1.00 mg/kg/day) doses of alendronate treatment (Allen and Burr, 2007). Finally, the model was used to predict the effects on remodeling and damage accumulation after 10 years of BP treatment to provide an understanding of longer term bisphosphonate use at periods similar to those for human osteoporosis patients.

Comparisons of simulation predictions to experimental results were made by examining the similarity of the values in comparison to the measured standard deviation and by a one sample t-test ( $p < 0.05$  significant) with the hypothesis that the simulation values represent the experimental means.

### Results

As expected, the simulated results following 1 year of BP treatment are consistent with experimental measurements (Table 4). At 1 year, the model predicts that the high dose of ALN will suppress Ac.f by 85% compared to 62% for the low dose. The equivalent values predicted for RIS are much more widely spread at 87% and 39%, respectively (Fig. 1). At the doses used for treatment of human post-menopausal osteoporosis, ALN (0.20 mg/kg/day) and RIS (0.10 mg/kg/day) reduce the number of active BMUs per year to 0.45 and 0.65, respectively. The model predicts that 1 year of ALN treatment increases BV/TV approximately 13% (Fig. 2) compared to 9.7 to 13% for RIS, depending on dose (Fig. 3). Microdamage is predicted to reach its maximum within the first year for the low dose of ALN (Fig. 2) or RIS (Fig. 3) treatment. For the middle and high doses of ALN and RIS, Cr.S.Dn is predicted to increase rapidly by 46 to 155% after 1 year of treatment. All predicted Ac.f, BV/TV, and Cr.S.Dn values at 1 year of treatment are within one standard deviation of their corresponding experimental measurements. The t-test analysis indicates a similarity between experimental results and their corresponding model predictions for all values at 1 year of BP treatment except for Ac.f for ALN at the high dose ( $p = 0.03$ ) and Cr.S.Dn for RIS at the low dose ( $p = 0.02$ ).

The model predicts modest additional increases in bone volume fraction between 1 and 3 years of treatment (Table 5). For ALN, the percent increase in BV/TV from the 1 year predictions ranges from 4.2% at the low dose to 5.2% at the high dose (Fig. 2). For RIS, the increase in



BV/TV ranges from 1.5% to 4.5% between the low and high doses, respectively (Fig. 3). In addition, the simulation predicts slight changes in Ac.f for ALN (-0.72% to -2.6%) and RIS (-1.5% to 3.4%) between 1 and 3 years of treatment.

Due to the bisphosphonate-induced inhibition of remodeling, resulting in a greater initial decline in the damage removal rate than the damage formation rate (Fig. 4), microdamage is predicted to increase during the first year of treatment. Within three years, Cr.S.Dn reaches its maximum value and thereafter trends downward at greatly varying rates depending on the dosage of ALN or RIS (Figs. 2 and 3). Compared to 1 year of treatment, the model predicts a 26% decrease in Cr.S.Dn after 3 years of low dose (0.05 mg/kg/day) RIS treatment. Under the high dose RIS regimen, Cr.S.Dn continues to increase throughout the second year and starts to diminish in the third year of treatment, reaching a damage burden at 3 years that is 20% above that at 1 year. The dynamics are similar for ALN, and for both bisphosphonates the maximum amounts of Cr.S.Dn predicted at 3 years increase with increasing dosage. For both ALN and RIS, the lowest dose allows a faster return to a low damage burden compared to the higher doses.

Predicted BV/TV, Cr.S.Dn, and Ac.f results at 3 years of treatment are at or within one standard deviation of the corresponding experimental measurements in all cases except for Ac.f at the middle dose of ALN which is 2.8 standard deviations different. The statistical analysis indicates significant differences for experimental results compared to predicted values for the middle dose ( $0 < p < 0.02$ ) but similarities for all values at the high dose after 3 years of treatment.

Depending on dose, the model predicts long term bisphosphonate treatment for 10 years to produce BV/TV increases of 20 to 29% for ALN (Fig. 2a) and 11 to 27% for RIS (Fig. 3a) compared to controls. Running the present model out to 10 years of treatment produces steady state values of Ac.f after approximately 2.5 years for RIS (Fig. 3c) and 3.5 years for ALN (Fig. 2c) that are 64 to 86% below the untreated controls for ALN and 36 to 88% below controls for RIS depending on dose. Microdamage accumulation (Figs. 2b and 3b) is also dose dependent and reaches its peak between 0.3 and 2.5 years (more quickly for lower doses). Microdamage reaches a steady state value ( $0.0093 \text{ mm/mm}^2$ ) slightly below the untreated controls after 8 years of ALN treatment for the low dose. After 10 years of the high dose RIS treatment, Cr.S.Dn ( $0.0233 \text{ mm/mm}^2$ ) is greater than those of the middle ( $0.0105 \text{ mm/mm}^2$ ) and low ( $0.0100 \text{ mm/mm}^2$ ) dose treatments. With the middle and high doses of ALN or the high dose of RIS, Cr.S.Dn continues to decline even after 10 years of treatment.

## Discussion

Bisphosphonates are widely used to treat human post-menopausal osteoporosis and have well-established anti-fracture efficacy. Experiments on canines involving 1 year of bisphosphonate treatment at various doses (including those used to treat post-menopausal osteoporosis) show suppressed bone remodeling activity; increased bone volume fraction, mineralization, stiffness, and microdamage accumulation; and reduced bone toughness (Mashiba *et al.*, 2001; Komatsubara *et al.*, 2003; Allen *et al.*, 2006). The goal of the current study was to develop a computational model to simulate the effects of BPs on bone remodeling based on 1 year experimental data from canine vertebrae and then examine results simulating long term BP use.

For varying doses of ALN or RIS, our model predicts a sharp decline in activation frequency during the first two months of treatment. Subsequently, Ac.f increases slightly, reaching a new equilibrium after 2 to 5 years of treatment. The degree of Ac.f decline is consistent with 1 year experimental data (Allen *et al.*, 2006), and its predicted long term steady state results are dose

dependent, with the three doses of RIS having a wider variation in long term results compared to the ALN doses.

In the simulation, microdamage accumulates rapidly within the first three years of BP treatment. Although the microdamage formation rate initially decreases sharply as a result of increases in BV/TV, which reduces the strain level in the representative bone volume, the initial decrease in the damage removal rate due to the Ac.f reduction is greater (Fig. 4). Then Ac.f and, subsequently, the damage removal rate begin to recover. Eventually, within 0.3 to 2.5 years depending on dose, the damage removal rate surpasses the diminished damage formation rate, and the burden of damage due to remodeling inhibition declines. These data predict that microdamage accumulation will be of greatest concern in the short-term following the initiation of BP treatment, prior to the point where bone volume increases sufficiently to reduce local strain. This is consistent with data from the 1 and 3 year experiments that show a significant increase in damage at 1 year but no difference between 1 and 3 years of ALN treatment (Allen and Burr, 2007). These results suggest that the reduced level of remodeling may be sufficient to control microdamage accumulation during long term BP treatment. The model predicts that ultimately, after 8 years of ALN treatment for the low dose, a new equilibrium is reached with a damage burden about 31% lower than that of the untreated baseline controls. For RIS the return to a steady state requires approximately 3 to 8 years for the low and middle doses, with damage at 10 years predicted to be 26% less for the low dose and 22% less for the middle dose relative to baseline controls.

One of the strengths of the current study is the ability to compare the simulation results with those from a well-designed experiment with control animals to represent the equilibrium status before BP treatment. Data on the effects of BP treatment on BV/TV, Ac.f, and Cr.S.Dn provide a foundation for defining the “dose-response coefficients” for the effects of the bisphosphonates examined. That the present model reasonably predicts the 3 year experimental work demonstrates the appropriateness of the coefficients chosen for the simulation and forms a basis to explore BP effects over time periods consistent with post menopausal life spans.

However, the present work clearly has significant limitations. The bone remodeling process is simplified in the model. For example, variability in the size and shape of resorption cavities, and many other aspects of the remodeling process, are not represented in the present computer simulation. Furthermore, the present model only simulates bone volume fraction as governed by remodeling within trabecular bone, and does not consider the microarchitecture of trabecular bone or the effects of cortical bone. Neither does it consider bone modeling activities that may affect bone fragility (Frost, 1998). The effects of remodeling are only considered with regard to elastic modulus; certainly bisphosphonates are expected to affect strength and toughness as well.

Experimental results show increased trabecular bone stiffness after BP treatment, but no difference in elastic modulus, ultimate load, or ultimate stress (Allen *et al.*, 2006). However, our simulation results indicate 1 year of BP treatment increases not only BV/TV but also elastic modulus in ALN- and RIS-treated animals compared to controls. One explanation for this discrepancy is that the effects of BP treatment on the degree of bone mineralization (Allen *et al.*, 2006), which significantly affects elastic modulus and other mechanical properties (Moore and Gibson, 2002; Wang and Niebur, 2006), was not considered in the model.

Over time, many of these limitations may be overcome by developing more detailed models in conjunction with ongoing experimental work and the accumulation of human data. In the meantime, the present simulation and experimental results suggest that the effects of bisphosphonates on bone remodeling may not lead to bone fragility associated with microdamage accumulation, and are consistent in that regard with ten year alendronate



treatment data for humans (Bone *et al.*, 2004). Further work is needed, however, before this and other clinical questions can be answered.

## Acknowledgments

This work was supported by NIH Grants R01 AR51555, R01 AR047838, and T32 AR007581, and a research grant from The Alliance for Better Bone Health (Procter and Gamble Pharmaceuticals and Sanofi-Aventis). Merck and Co. kindly provided the alendronate. This investigation utilized an animal facility constructed with support from Research Facilities Improvement Program Grant Number C06RR10601 from the NIH National Center for Research Resources.

## References

- Allen MR, Burr DB. Three years of alendronate treatment results in similar levels of vertebral microdamage as after one year of treatment. *Journal of Bone and Mineral Research* 2007;22(11):1759–1765. [PubMed: 17663638]
- Allen MR, Iwata K, Phipps R, Burr DB. Alterations in canine vertebral bone turnover, microdamage accumulation, and biomechanical properties following 1-year treatment with clinical treatment doses of risedronate and alendronate. *Bone* 2006;39(4):872–879. [PubMed: 16765660]
- Beaupre GS, Orr TE, Carter DR. An approach for time-dependent bone modeling and remodeling-application: a preliminary remodeling simulation. *Journal of Orthopaedic Research* 1990;8(5):662–670. [PubMed: 2388106]
- Boivin GY, Chavassieux PM, Santora AC, Yates J, Meunier PJ. Alendronate increases bone strength by increasing the mean degree of mineralization of bone tissue in osteoporotic women. *Bone* 2000;27(5):687–694. [PubMed: 11062357]
- Bone HG, Hosking D, Devogelaer JP, Tucci JR, Emkey RD, Tonino RP, Rodriguez-Portales JA, Downs RW, Gupta J, Santora AC, Liberman UA. Alendronate Phase III Osteoporosis Treatment Study Group. Ten years' experience with alendronate for osteoporosis in postmenopausal women. *New England Journal of Medicine* 2004;350(12):1189–1199. [PubMed: 15028823]
- Borah B, Dufresne TE, Ritman EL, Jorgensen SM, Liu S, Chmielewski PA, Phipps RJ, Zhou X, Sibonga JD, Turner RT. Long-term risedronate treatment normalizes mineralization and continues to preserve trabecular architecture: sequential triple biopsy studies with micro-computed tomography. *Bone* 2006;39(2):345–352. [PubMed: 16571382]
- Boyce RW, Paddock CL, Gleason JR, Sletsema WK, Eriksen EF. The effects of risedronate on canine cancellous bone remodeling: three-dimensional kinetic reconstruction of the remodeling site. *Journal of Bone and Mineral Research* 1995;10(2):211–221. [PubMed: 7754801]
- Burr DB, Martin RB, Schaffler MB, Radin EL. Bone remodeling in response to in vivo fatigue microdamage. *Journal of Biomechanics* 1985;18:189–200. [PubMed: 3997903]
- Chavassieux PM, Arlot ME, Reda C, Wei L, Yates AJ, Meunier PJ. Histomorphometric assessment of the long-term effects of alendronate on bone quality and remodeling in patients with osteoporosis. *Journal of Clinical Investigation* 1997;100:1475–1480. [PubMed: 9294113]
- Chavassieux PM, Arlot ME, Roux JP, Portero N, Daifotis A, Yates AJ, Hamdy NA, Malice MP, Freedholm D, Meunier PJ. Effects of alendronate on bone quality and remodeling in glucocorticoid-induced osteoporosis: a histomorphometric analysis of transiliac biopsies. *Journal of Bone and Mineral Research* 2000;15:754–762. [PubMed: 10780867]
- Day JS, Ding M, Bednarz P, van der Linden JC, Mashiba T, Hirano T, Johnston CC, Burr DB, Hvid I, Sumner DR, Weinans H. Bisphosphonate treatment affects trabecular bone apparent modulus through micro-architecture rather than matrix properties. *Journal of Orthopaedic Research* 2004;22(3):465–471. [PubMed: 15099622]
- Delmas PD. How does antiresorptive therapy decrease the risk of fracture in women with osteoporosis? *Bone* 2000;27:1–3. [PubMed: 10865202]
- Ding M, Day JS, Burr DB, Mashiba T, Hirano T, Weinans H, Sumner DR, Hvid I. Canine cancellous bone microarchitecture after one year of high-dose bisphosphonates. *Calcified Tissue International* 2003;72(6):737–744. [PubMed: 14563003]
- Dufresne TE, Chmielewski PA, Manhart MD, Johnson TD, Borah B. Risedronate preserves bone architecture in early postmenopausal women in 1 year as measured by three-dimensional

- microcomputed tomography. *Calcified Tissue International* 2003;73(5):423–432. [PubMed: 12964065]
- Eriksen EF, Melsen F, Sod E, Barton I, Chines A. Effects of long-term risedronate on bone quality and bone turnover in women with postmenopausal osteoporosis. *Bone* 2002;31:620–625. [PubMed: 12477578]
- Forwood MR, Burr DB, Takano Y, Eastman DF, Smith PN, Schwardt JD. Risedronate treatment does not increase microdamage in the canine femoral neck. *Bone* 1995;16(6):643–650. [PubMed: 7669441]
- Frost HM. Tetracycline-based histological analysis of bone remodeling. *Calcified Tissue International* 1969;3:211–237.
- Frost HM. Osteoporoses: a rationale for further definitions? *Calcified Tissue International* 1998;62(2): 89–94. [PubMed: 9437039]
- Hazelwood SJ, Martin RB, Rashid MM, Rodrigo JJ. A mechanistic model for internal bone remodeling exhibits different dynamic responses in disuse and overload. *Journal of Biomechanics* 2001;34:299–308. [PubMed: 11182120]
- Hirano T, Turner CH, Forwood MR, Johnston CC, Burr DB. Does suppression of bone turnover impair mechanical properties by allowing microdamage accumulation? *Bone* 2000;27(1):13–20. [PubMed: 10865204]
- Komatsubara S, Mori S, Mashiba T, Ito M, Li J, Kaji Y, Akiyama T, Miyamoto K, Cao Y, Kawanishi J, Norimatsu H. Long-term treatment of incadronate disodium accumulates microdamage but improves the trabecular bone microarchitecture in dog vertebra. *Journal of Bone and Mineral Research* 2003;18 (3):512–520. [PubMed: 12619936]
- Komatsubara S, Mori S, Mashiba T, Li J, Nonaka K, Kaji Y, Akiyama T, Miyamoto K, Cao Y, Kawanishi J, Norimatsu H. Suppressed bone turnover by long-term bisphosphonate treatment accumulates microdamage but maintains intrinsic material properties in cortical bone of dog rib. *Journal of Bone and Mineral Research* 2004;19:999–1005. [PubMed: 15125797]
- Martin RB. The usefulness of mathematical models for bone remodeling. *Yearbook of Physical Anthropology* 1985;28:227–236.
- Martin RB. Mathematical model for repair of fatigue damage and stress fracture in osteonal bone. *Journal of Orthopaedic Research* 1995;13:309–316. [PubMed: 7602391]
- Mashiba T, Hirano T, Turner CH, Forwood MR, Johnston CC, Burr DB. Suppressed bone turnover by bisphosphonates increases microdamage accumulation and reduces some biomechanical properties in dog rib. *Journal of Bone and Mineral Research* 2000;15(4):613–620. [PubMed: 10780852]
- Mashiba T, Mori S, Burr DB, Komatsubara S, Cao Y, Manabe T, Norimatsu H. The effects of suppressed bone remodeling by bisphosphonates on microdamage accumulation and degree of mineralization in the cortical bone of dog rib. *Journal of Bone and Mineral Research* 2005;23(Supplement):36–42.
- Mashiba T, Turner CH, Hirano T, Forwood MR, Johnston CC, Burr DB. Effects of suppressed bone turnover by bisphosphonates on microdamage accumulation and biomechanical properties in clinically relevant skeletal sites in beagles. *Bone* 2001;28:524–531. [PubMed: 11344052]
- Miller PD, Watts NB, Licata AA, Harris ST, Genant HK, Wasnich RD, Ross PD, Jackson RD, Hoseyni MS, Schoenfeld SL, Valent DJ, Chesnut CHR. Cyclical etidronate in the treatment of postmenopausal osteoporosis: efficacy and safety after seven years of treatment. *American Journal of Medicine* 1997;103(6):468–476. [PubMed: 9428829]
- Moore TLA, Gibson LJ. Microdamage accumulation in bovine trabecular bone in uniaxial compression. *Journal of Biomechanical Engineering-Transactions of the ASME* 2002;124(1):63–71.
- Mori S, Burr DB. Increased intracortical remodeling following fatigue damage. *Bone* 1993;14:103–109. [PubMed: 8334026]
- Nyman JS, Rodrigo JJ, Hazelwood SJ, Yeh OC, Martin RB. Predictions on preserving bone mass in knee arthroplasty with bisphosphonates. *Journal of Arthroplasty* 2006;21(1):106–113. [PubMed: 16446194]
- Nyman JS, Yeh OC, Hazelwood SJ, Martin RB. A theoretical analysis of long-term bisphosphonate effects on trabecular bone volume and microdamage. *Bone* 2004;35:296–305. [PubMed: 15207770]
- Porras AG, Holland SD, Gertz BJ. Pharmacokinetics of alendronate. *Clinical Pharmacokinetics* 1999;36:315–328. [PubMed: 10384857]

- Recker RR, Gallagher R, MacCosbe PE. Effect of dosing frequency on bisphosphonate medication adherence in a large longitudinal cohort of women. *Mayo Clinic Proceedings* 2005;80(7):856–861. [PubMed: 16007889]
- Rodan GA, Fleisch HA. Bisphosphonates: mechanisms of action. *Journal of Clinical Investigation* 1996;97(12):2692–2696. [PubMed: 8675678]
- Schaffler MB, Choi K, Milgrom C. Aging and matrix microdamage accumulation in human compact bone. *Bone* 1995;17:521–525. [PubMed: 8835305]
- Ste-Marie LG, Sod E, Johnson T, Chines A. Five years of treatment with risedronate and its effects on bone safety in women with postmenopausal osteoporosis. *Calcified Tissue International* 2004;75(6):469–476. [PubMed: 15478000]
- Storm T, Steiniche T, Thamsborg G, Melsen F. Changes in bone histomorphometry after long-term treatment with intermittent, cyclic etidronate for postmenopausal osteoporosis. *Journal of Bone and Mineral Research* 1993;8:199–208. [PubMed: 8442438]
- Tonino RP, Meunier PJ, Emkey R, Rodriguez-Portales JA, Menkes CJ, Wasnich RD, Bone HG, Santora AC, Wu M, Desai R, Ross PD. Skeletal benefits of alendronate: 7-year treatment of postmenopausal osteoporotic women. Phase III Osteoporosis Treatment Study Group. *Journal of Clinical Endocrinology and Metabolism* 2000;85(9):3109–3115. [PubMed: 10999794]
- Wang X, Niebur GL. Microdamage propagation in trabecular bone due to changes in loading mode. *Journal of Biomechanics* 2006;39:781–790. [PubMed: 16488217]
- Whalen RT, Carter DR, Steele CR. Influence of physical activity on the regulation of bone density. *Journal of Biomechanics* 1988;21(10):825–837. [PubMed: 3225269]
- Zoehrer R, Roschger P, Paschalis EP, Hofstaetter JG, Durchschlag E, Fratzl P, Phipps R, Klaushofer K. Effects of 3- and 5-year treatment with risedronate on bone mineralization density distribution in triple biopsies of the iliac crest in postmenopausal women. *Journal of Bone and Mineral Research* 2006;21(7):1106–1112. [PubMed: 16813531]

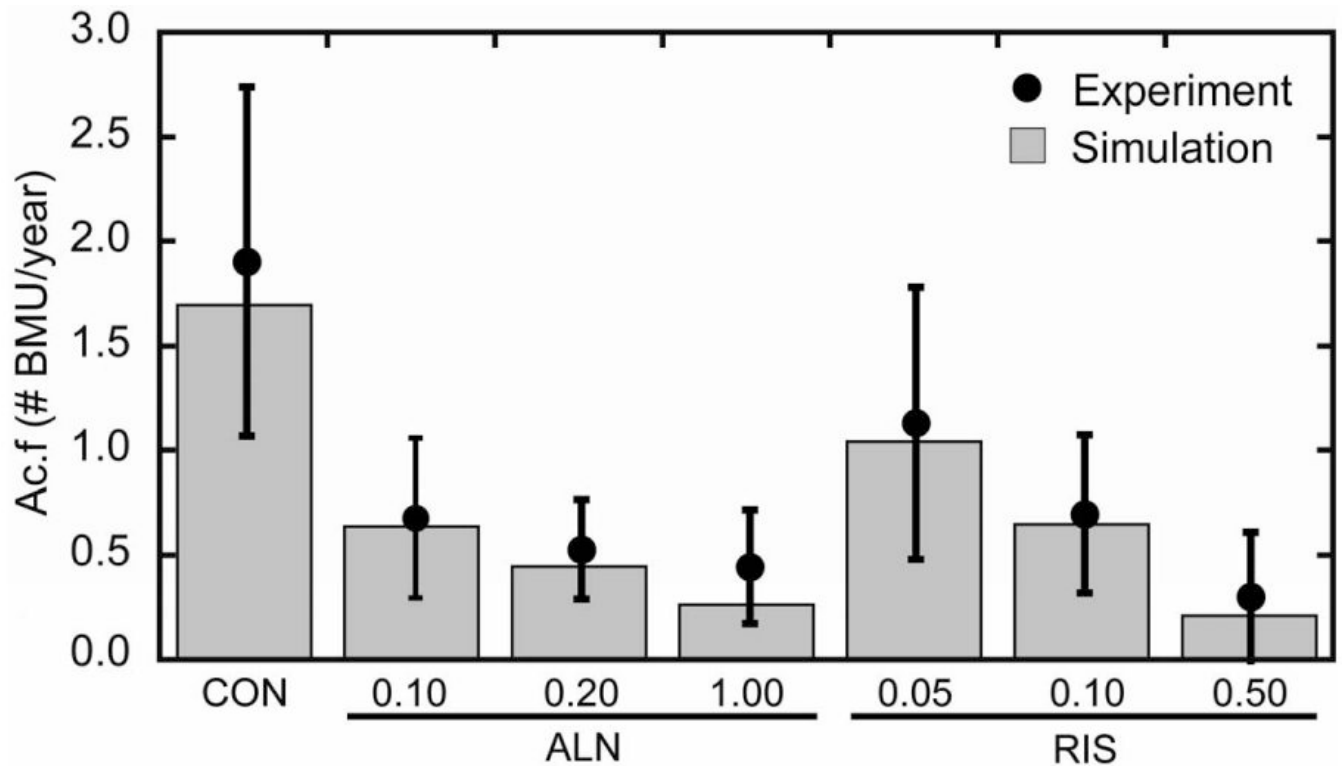


**Figure 1.**

Ac.f<sub>year</sub> decreases in relation to control after 1 year of ALN and RIS treatment. The error bars represent one standard deviation. CON represents the control data. ALN 0.10 refers to an alendronate dose of 0.10 mg/kg/day, etc.

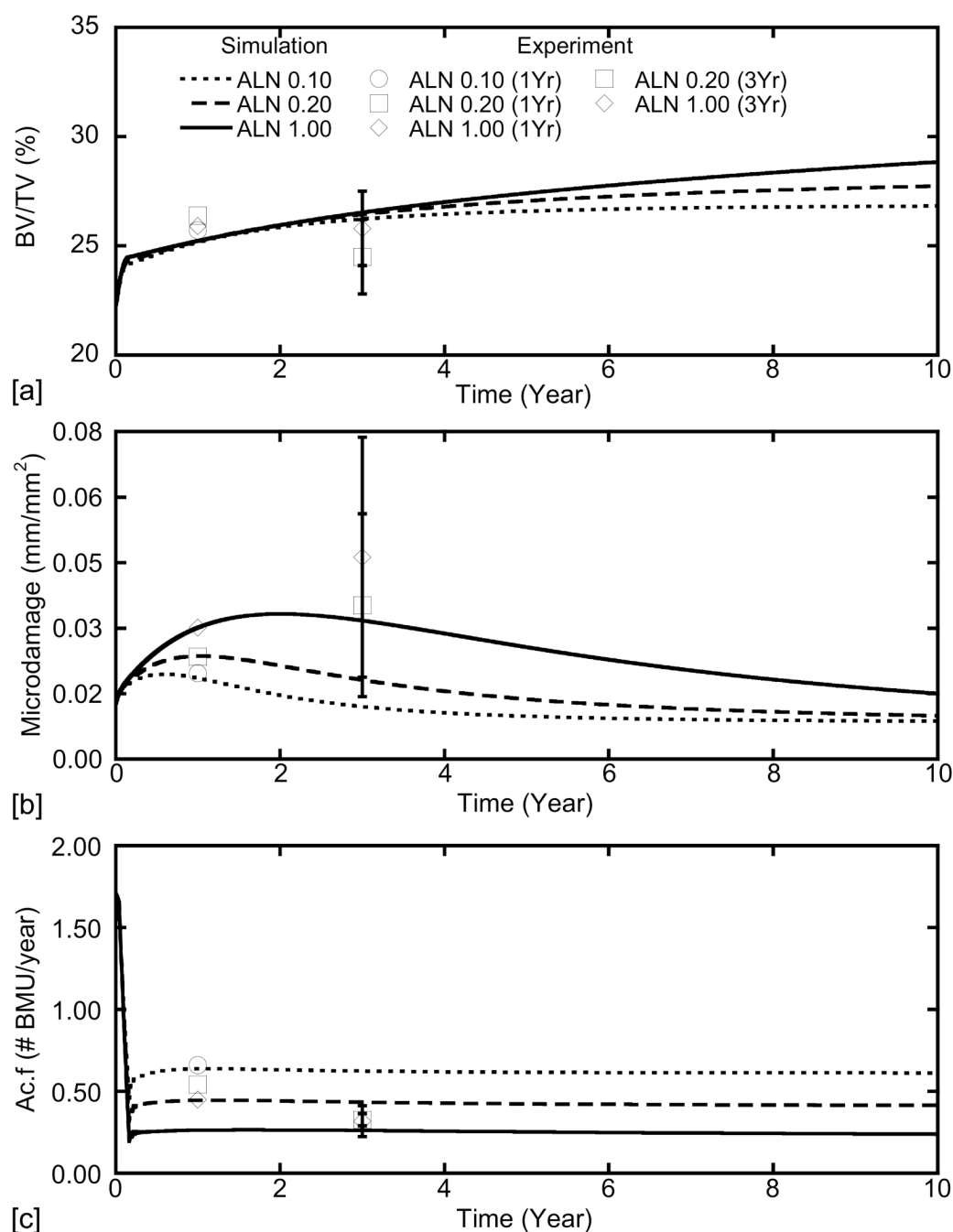


**Figure 2.**

Predictions for BV/TV, Cr.S.Dn and Ac.f during 3 years of ALN treatment. Time=0 represents the beginning of ALN treatment. ALN 0.10 refers to an alendronate dose of 0.10 mg/kg/day, etc. The error bars represent  $\pm 1$  standard deviation.

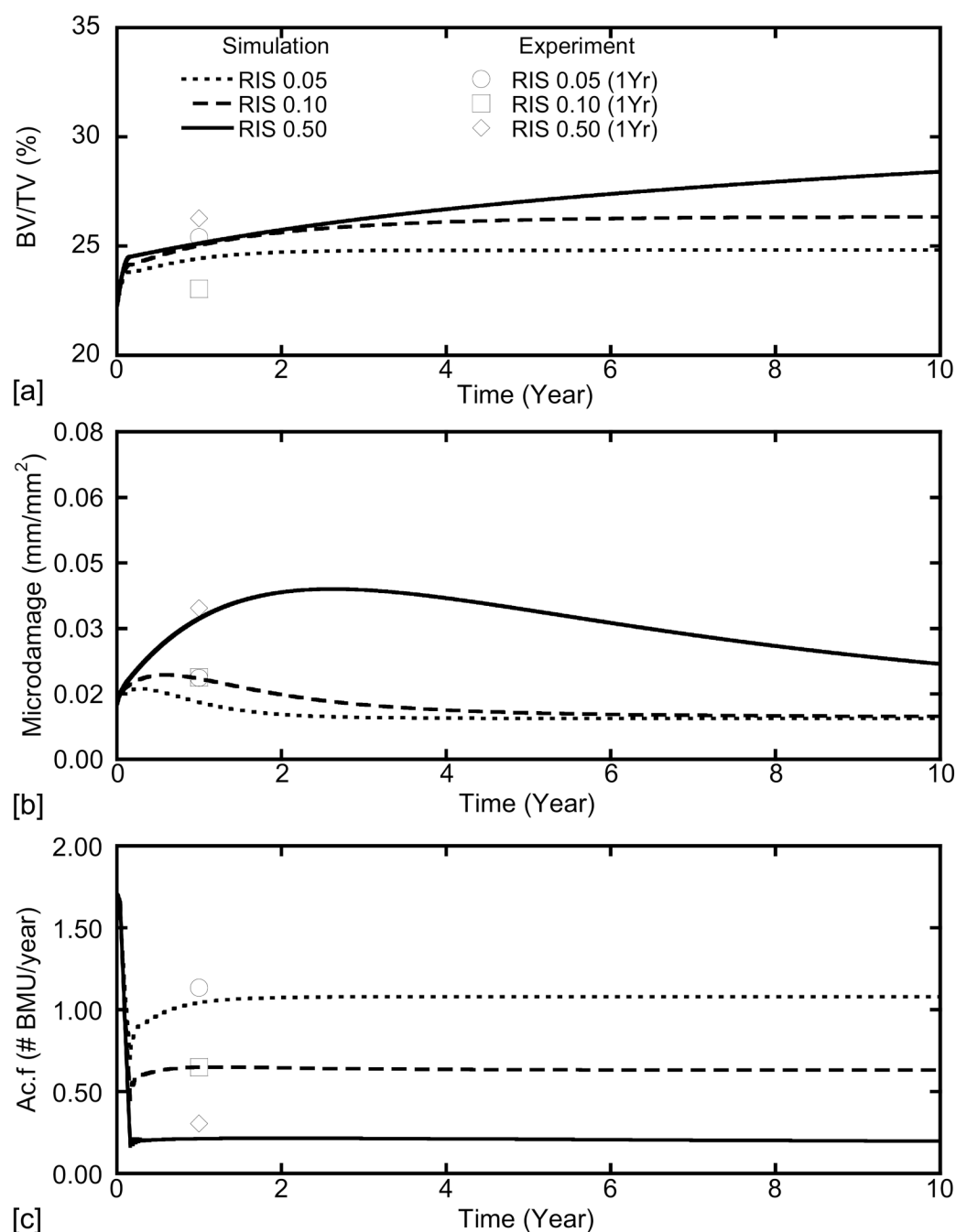


**Figure 3.** Predictions for BV/TV, Cr.S.Dn and Ac.f during 3 years of RIS treatment. Time=0 represents the beginning of RIS treatment. RIS 0.05 refers to a risedronate dose of 0.05 mg/kg/day, etc.



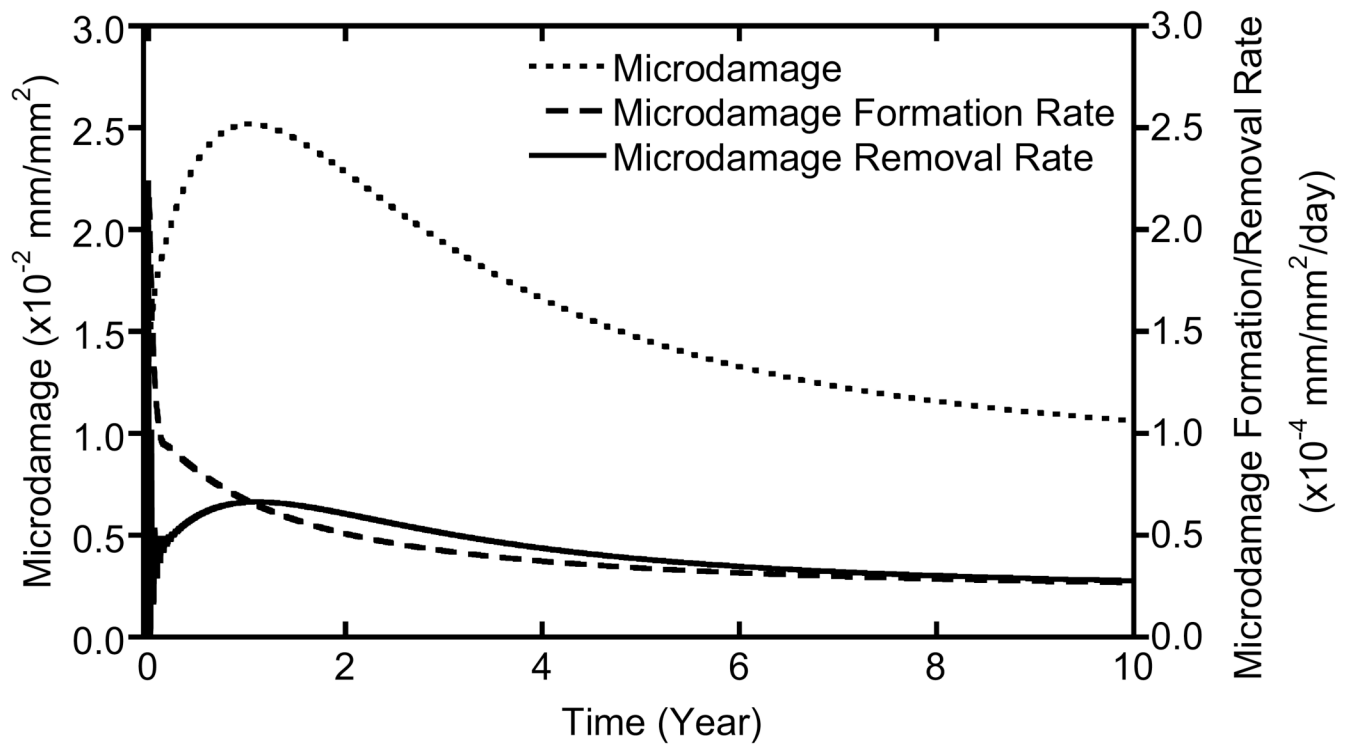


**Figure 4.**

In the dogs subjected to the middle dose of ALN (0.20 mg/kg/day), the simulation predicts that microdamage formation and removal rates initially decrease sharply after BP administration. As the microdamage formation rate continues to decline over time due to further increases in BV/TV, the damage removal rate recovers as a result of increases in Ac.f. As the microdamage removal rate surpasses the formation rate, damage accumulation declines. Similar patterns were observed for all doses of ALN and RIS.

**Table 1**

Model state variables

	State variable
E	Elastic modulus (MPa)
BV/TV	Volume fraction
N.Rs.BMU	Number of resorbing BMUs (# BMU/mm <sup>2</sup> )
N.F.BMU	Number of refilling BMUs (# BMU/mm <sup>2</sup> )
Ac.f	BMU activation frequency (# BMU/mm <sup>2</sup> /day)
Ac.f <sub>year</sub>	BMU activation frequency (# BMU/year)
BS/TA	Bone surface area per section area
Cr.S.Dn	Microdamage (mm/mm <sup>2</sup> )
$\sigma$	Peak stress of cyclic compressive loading
$\varepsilon$	Peak strain of cyclic compressive loading
$\Phi$	Mechanical stimulus (cycles per day, cpd)

**Table 2**

## Model constants

	Constant	Values	Source
$E_0$	Tissue modulus (MPa)	19735	Calculated <sup>*</sup>
$b$	Modulus-BV/TV exponent	2.4217	Calculated <sup>*</sup>
$Rs.Ar$	Resorption area, mm <sup>2</sup>	0.01395	Measured <sup>*</sup>
$F.Ar$	Refilling area, mm <sup>2</sup>	0.01395	Assumed equal to $Rs.Ar$
$C_F$	Ratio of $F.Ar$ to $Rs.Ar_{(BP)}$	1.45-2	-
$Rs.Ar_{(BP)}$	BP treatment resorption area, mm <sup>2</sup>	$F.Ar/C_F$	-
$E.De$	Erosion cavity depth, mm	0.0667	Measured <sup>*</sup>
$E.Wi$	Erosion cavity width, mm	0.293	Measured <sup>*</sup>
$Md.S.Le$	Mean mineralized bone surface length, mm	0.1935	Measured <sup>*</sup>
$Rs.P$	Resorption period, days	10	Measured <sup>*</sup>
$Rv.P$	Reversal period, days	5	(Nyman <i>et al.</i> , 2004)
$FP$	Refilling period, days	44	Measured <sup>*</sup>
$k_D$	Damage rate coefficient, mm/mm <sup>2</sup>	$11 \times 10^5$	Estimated <sup>**</sup>
$q$	Damage rate exponent	4	(Whalen <i>et al.</i> , 1988; Hazelwood <i>et al.</i> , 2001)
$R_L$	Loading rate, cpd	3000	(Hazelwood <i>et al.</i> , 2001)
$F_s$	Damage removal specificity factor	20	Estimated <sup>**</sup>
$Cr.S.Dn_0$	Threshold damage, mm/mm <sup>2</sup>	0.01	Estimated <sup>**</sup>
$Ac.f_0$	Threshold BMU act. freq., BMUs/mm <sup>2</sup> /day	0.08	Estimated <sup>**</sup>
$\Phi_0$	Threshold mechanical stimulus, cpd	$1.875 \times 10^{-10}$	(Beaupre <i>et al.</i> , 1990)
$Ac.f_{max}$	Max. BMU act. freq., BMUs/mm <sup>2</sup> /day	0.50	(Frost, 1969; Schaffler <i>et al.</i> , 1995)
$k_b$	Act. freq. dose-response coefficient, cpd <sup>-1</sup>	$6.5 \times 10^{10}$	(Hazelwood <i>et al.</i> , 2001)
$k_c$	Act. freq. dose-response coefficient, cpd	$9.4 \times 10^{-11}$	(Hazelwood <i>et al.</i> , 2001)
$k_r$	Act. freq. coefficient	-1.6	(Hazelwood <i>et al.</i> , 2001)
$P_{max}$	Maximum potency	1	(Nyman <i>et al.</i> , 2004)
$\tau_s$	Coefficient	1-50	(Nyman <i>et al.</i> , 2004)

\* Previously unpublished data measured or calculated from the specimens of Allen et al. (2006).

\*\* Parameters estimated in the model simulation to produce steady state values for  $Ac.f$ ,  $Cr.S.Dn$ , and  $BV/TV$  similar to the remodeling data for controls and 1 year experiments.

**Table 3**

Sensitivity analysis of bisphosphonate effects simulated by the model

Bisphosphonate	Dosage (mg/kg/day)	Suppression Coeff. $\tau_s$	Refilling Coeff. $C_F$
ALN	0.10	11.3	1.70
	0.20	18.8	1.80
	1.00	38	2.00
RIS	0.05	5	1.45
	0.10	11	1.65
	0.50	50	2.00

**Table 4**

Model predictions and experimental measurements in the canine vertebral body after 1 year of ALN or RIS treatment.

Treatment	Variable	Simulation	Experiment
Control	BV/TV	0.223	0.219 ± 0.031
	Cr.S.Dn (mm/mm <sup>2</sup> )	0.0135	0.0068 ± 0.0073
	Ac.f <sub>year</sub> (# BMUs/year)	1.70	1.89 ± 0.84
1 year ALN 0.10 mg/kg/day	BV/TV	0.252	0.257 ± 0.052
	Cr.S.Dn	0.0198	0.0210 ± 0.0178
	Ac.f <sub>year</sub>	0.64	0.66 ± 0.38
1 year ALN 0.20 mg/kg/day	BV/TV	0.252	0.264 ± 0.036
	Cr.S.Dn	0.0252	0.0250 ± 0.0140
	Ac.f <sub>year</sub>	0.45	0.54 ± 0.24
1 year ALN 1.00 mg/kg/day	BV/TV	0.252	0.259 ± 0.044
	Cr.S.Dn	0.0321	0.0322 ± 0.0212
	Ac.f <sub>year</sub>	0.26	0.45 ± 0.27
1 year RIS 0.05 mg/kg/day	BV/TV	0.244	0.254 ± 0.038
	Cr.S.Dn	0.0140	0.0199 ± 0.0075
	Ac.f <sub>year</sub>	1.04	1.13 ± 0.65
1 year RIS 0.10 mg/kg/day	BV/TV	0.250	0.231 ± 0.038
	Cr.S.Dn	0.0197	0.0200 ± 0.0121
	Ac.f <sub>year</sub>	0.65	0.65 ± 0.38
1 year RIS 0.50 mg/kg/day	BV/TV	0.251	0.263 ± 0.037
	Cr.S.Dn	0.0344	0.0370 ± 0.0195
	Ac.f <sub>year</sub>	0.21	0.31 ± 0.31

**Table 5**

Model predictions for changes in the canine vertebral body after 3 years of ALN or RIS treatment

Treatment	Variable	Simulation	Change From 1 Year Simulation Result (%)	Experiment <sup>*</sup>
3 year ALN 0.10 mg/kg/day	BV/TV	0.262	4.21	-
	Cr.S.Dn (mm/mm <sup>2</sup> )	0.0128	-35.35	-
	Ac.f <sub>year</sub> (# BMU/year)	0.62	-2.25	-
3 year ALN 0.20 mg/kg/day	BV/TV	0.264	4.84	0.245 ± 0.017
	Cr.S.Dn	0.0193	-23.41	0.0376 ± 0.0223
	Ac.f <sub>year</sub>	0.43	-2.58	0.328 ± 0.037
3 year ALN 1.00 mg/kg/day	BV/TV	0.265	5.15	0.258 ± 0.017
	Cr.S.Dn	0.0338	5.30	0.0493 ± 0.0293
	Ac.f <sub>year</sub>	0.26	-0.72	0.319 ± 0.094
3 year RIS 0.05 mg/kg/day	BV/TV	0.248	1.47	-
	Cr.S.Dn	0.0103	-26.42	-
	Ac.f <sub>year</sub>	1.08	3.43	-
3 year RIS 0.10 mg/kg/day	BV/TV	0.259	3.59	-
	Cr.S.Dn	0.0133	-32.49	-
	Ac.f <sub>year</sub>	0.64	-1.49	-
3 year RIS 0.50 mg/kg/day	BV/TV	0.262	4.50	-
	Cr.S.Dn	0.0414	20.35	-
	Ac.f <sub>year</sub>	0.21	0.70	-

\* Three year experimental data are available for only the 0.20 mg/kg/day and 1.00 mg/kg/day ALN treatments (Allen and Burr, 2007).